Core-level x-ray photoemission on NiO in the impurity limit

S. Altieri and L. H. Tjeng
Solid State Physics Laboratory, Materials Science Centre, University of Groningen, Nijenborgh 4, 9747 AG Groningen, The Netherlands

A. Tanaka
Department of Materials Science, Faculty of Science, Hiroshima University, Higashi-Hiroshima 724, Japan

G. A. Sawatzky
Solid State Physics Laboratory, Materials Science Centre, University of Groningen, Nijenborgh 4, 9747 AG Groningen, The Netherlands
(Received 20 September 1999)

We present a core level X-ray photoelectron spectroscopy study of $Ni_xMg_{1-x}O$ crystals with $0.03<x<1$. We show that nonlocal effects involving inter-Ni-site fluctuations strongly influence the Ni $2p$ core-level spectra for higher Ni concentrations including NiO itself. It is only in the very dilute Ni limit that the core-level spectra can be described in terms of an Anderson impurity model which also must include a realistic band structure for the O $2p$. Moreover, it is only in this limit that a single-site model can explain the core-level and valence-band spectra as well as the optical data by using one consistent set of parameter values. These results consolidate the concepts of nonlocal screening and provide a better understanding of the electronic structure of NiO.

I. INTRODUCTION

Core-level x-ray photoelectron spectroscopy (XPS) is a powerful tool to study the electronic structure of strongly correlated systems.[1–5] In recent years, the use of core-level XPS in combination with single-site cluster or Anderson impurity calculations has led to a great progress in our understanding of transition metal (TM) compounds[6–9] and rare-earth (RE) materials.[10–13] After the discovery of the high-T_c superconductors, Cu $2p$ XPS was used to establish the strongly correlated nature of these systems, and has provided estimates for a number of important parameters such as the O $2p$ to Cu $3d$ charge-transfer energy (Δ) and the valence of the Cu in the CuO_2 planes.[14–19] However, the Anderson impurity approaches are not able to explain some important aspects like the large width of the Cu $2p$ main line in the cuprates,[14–17] or the double peak structure in the main line of the Ni $2p$ in NiO.[20–23] Moreover, in these single-site approaches, the values for Δ in TM and high-T_c compounds estimated from $2p$ XPS are systematically too low,[14–19] and the behavior of the Cu $2p$ spectra upon hole doping[16,17] is also not well understood.

Van Veenendaal and Sawatzky[24,25] have studied the effect of the interactions between different TM ions on these spectra, using calculations of clusters involving more than one TM ion, and a multiband Hubbard Hamiltonian. They showed that, besides the peaks of mainly $2p^53d^n$ and $2p^53d^{n+1}\underline{L}$ character typically found in the single-site approaches, where $\underline{L}$ denotes a hole in the oxygen valence band, a different peak of mainly $2p^53d^{n+1}$ appears in the XPS spectrum, due to the transfer of a hole from the ligand of the core ionized site to the ligands of a next neighbor cluster, where a Zhang-Rice singlet state[26,27] is formed. This intersite charge-transfer screening mechanism explains the $2p$ main line of CuO and the high T_c's, the Ni $2p$ line shape of NiO, and also the changes induced by different Ni local environments.[28] Many experimental[29–31] and theoretical[32–40] studies are now being carried out to study the effect of the cluster size on core-level photoemission, photoabsorption, and x-ray emission spectra of various Cu and Ni compounds.

In the last several years, however, a large number of alternative explanations have been proposed for this $2p$ core level line-shape problem, all starting from a local ansatz. Karlsson, Gunnarsson, and Jepsen[40,41] inserted the valence-band structure as a possible explanation for the variations in the Cu $2p$ line shape. Others suggested that the double peak structure in the main line of the Ni $2p$ in NiO is a result of the presence of both the $2p^53d^9\underline{L}$ and $2p^53d^{10}\underline{L}^2$ configurations.[21] Very recently, Parmigiani and co-workers noticed that structures similar to those observed in the Ni $2p$, and ascribed by van Veenendaal and Sawatzky to nonlocal screening processes, are also present in the Ni $3s$ XPS.[42] Since the experimental $3s$ spectrum can be well reproduced by *ab initio* Hartree-Fock calculations[43] or Anderson impurity calculations,[44,45] they concluded that intersite screening effects are not needed. In fact, based on their analysis of the $2p_{1/2}$ spectrum of La_2NiO_4,[42] they claimed that these effects are even nonexistent for Ni^{2+} compounds.

In order to determine the applicability limits of the very different theories, an experiment is necessary which allows one to isolate the basic physics underlying the different approaches. This can be done, for example, by studing XPS spectra of highly diluted TM impurities in a MgO matrix. In this case, nonlocal screening effects are inhibited due to the absence of neighbor TM ions, and the TM core-level XPS will be influenced exclusively by charge-transfer processes from the nearest-neighbor oxygen atoms, and, possibly, by oxygen banding effects.

Core-level XPS spectra from powdered samples of Ni^{2+} impurities in MgO, with concentrations ranging from 9 to 47%, have been reported more than 20 years ago.[46] A Ni $2p$

spectrum of a $Ni_{0.1}Mg_{0.9}O$ sample has also been published more recently.[4] Both sets of data show that the Ni $2p$ main line consists of a single peak, in contrast to the double peak structure for bulk NiO. It was, however, contended by Sangaletti, Depero, and Parmigiani[42] that the width of the main line of these diluted NiO samples is as large as that of the NiO single-crystal material, so that those data do not support the nonlocal screening model for bulk NiO. It was also pointed out by Hüfner[4] that the peak position of the Ni $2p$ of the diluted sample with respect to that of the bulk NiO seems to be contrary to expectations. It is conceivable that these apparent contradictions are caused by charging problems that occur during the measurements of these highly insulating materials. In addition, the lowest Ni concentration studied was $\approx 10\%$, implying that the probability[47] for two Ni ions to be neighbors with a 180° Ni-O-Ni bond angle was $\approx 35\%$, i.e., still too high to exclude the presence of possible strong nonlocal screening in the XPS final state.

In this paper, we present a high-resolution core-level XPS study of $Ni_xMg_{1-x}O$ crystals with $0.03<x<1$, grown epitaxially on a Ag(100) substrate. We will show that in the dilute limit the XPS spectra are properly described by an Anderson impurity Hamiltonian including the full multiplet structure, and that the inclusion of a realistic band structure for the O $2p$ states is necessary. We will also show that in bulk NiO, the Ni $2p$ spectral line shapes are strongly influenced by the interaction with neighboring Ni ions. And finally we will demonstrate that it is only in the dilute limit that the single-site model can explain the core-level and valence-band spectra as well as the optical data by using one consistent set of parameter values.

II. EXPERIMENT

The XPS spectra presented in this paper have been recorded at room temperature in a Vacuum Generators (VG) Surface Science X-probe spectrometer unit, equipped with a small spot (150–1000 μm) Al-K_α source ($h\nu = 1486.6$ eV) monochromatized by a VG twin crystal, and with a hemispherical electron energy analyzer with multichannel detection system. The XPS overall energy resolution was 0.5 eV, as determined using the Fermi cutoff of a Ag reference sample. The zero of the binding energy scale was given by the Fermi level of this Ag reference. The photoelectrons were collected at a takeoff angle of 55° with respect to the surface normal of the samples. The base pressure in the spectrometer was 5×10^{-11} mbar, and the pressure raised to 1.5×10^{-10} during the measurements due to the operation of the x-ray source. While charging effects usually hamper seriously the XPS measurements of wide band-gap insulators like MgO, it turned out that such effects were not observed for the thin $Ni_xMg_{1-x}O$ films grown on Ag(100).

The films were prepared *in situ* in an attached ultrahigh vacuum (UHV) preparation chamber, equipped with a reflection high-energy electron-diffraction (RHEED) system to monitor the structural quality and thickness of the epitaxial films, and operating under the conditions as determined by the experiments in a previous work for the epitaxial growth of stoichiometric MgO(100) and NiO(100) films on the Ag(100) substrate.[48–50] The $Ni_xMg_{1-x}O$ films with a thickness varying between 40 and 80 Å were grown by co-evaporating high-purity Mg and Ni metals from two different Luxel Radak-I effusion cells onto a clean and ordered Ag(100), and simultaneously dosing molecular oxygen from a nozzle. The Mg effusion cell temperature was set at about 330 °C to obtain a MgO growth rate of about one monolayer per minute, as determined from the period of the intensity oscillations of the RHEED pattern.[50] The Ni effusion cell temperature was tuned from 1095 to 1230 °C to obtain Ni impurities in the MgO matrix with concentrations ranging from 1% up to 53%, as determined by comparing the O $1s$ to Ni $2p$ core-level intensity ratio with that of a NiO single crystal reference sample cleaved *in situ*. The films are then capped by a layer of pure MgO of about 5 Å thick, in order to minimize undesired surface effects on the measured Ni core-level spectra.

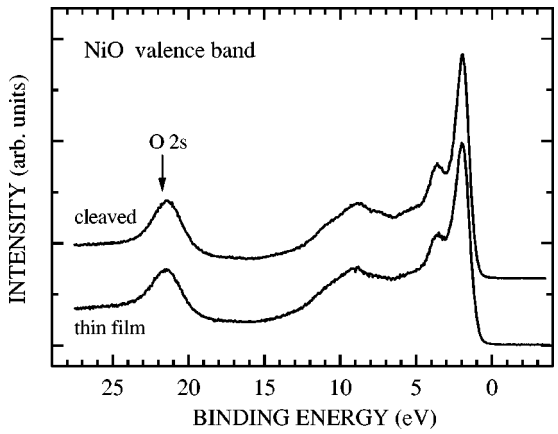

FIG. 1. Valence-band XPS spectra measured from an *in situ* cleaved NiO single crystal (top) and from a 120-Å-thick NiO film grown on polycrystalline Al (bottom). Note the close similarity between the two spectra.

The base pressure of the preparation chamber was 2×10^{-10} mbar. With the nozzle positioned close to the sample (≈ 5 cm), a background O_2 pressure of $\approx 3\times10^{-7}$ mbar was more than sufficient to ensure full oxidation of the co-evaporated Mg and Ni to MgO and NiO, respectively. The Ag substrate temperature was kept at room temperature during the overlayer growth. For reference purposes an Al polycrystalline substrate was also used, as well as a bulk MgO sample, which was prepared by cleaving a MgO slab of a few millimeters thick in air to expose a fresh (100) surface and successively annealing it *in situ* for 8 h at 600°C in a O_2 atmosphere of 1×10^{-6} mbar.

III. RESULTS

To verify the quality of the films, we first grew pure NiO and MgO films using the evaporation technique described in the previous section. We found that the Ni $2p$ to O $1s$ XPS and the Mg $KL_{2,3}L_{2,3}$ Auger to O $1s$ XPS intensity ratios of the films are identical with those of the cleaved NiO and MgO single crystals, respectively, indicating that the composition is indeed stoichiometric. For a more detailed investigation, we have measured the valence-band XPS spectrum from a 120-Å-thick NiO film supported on Al, as shown in the bottom panel of Fig. 1. For the valence band we have used Al instead of Ag as substrate since otherwise the substrate Ag $4d$ may spuriously contribute to the oxide spec-

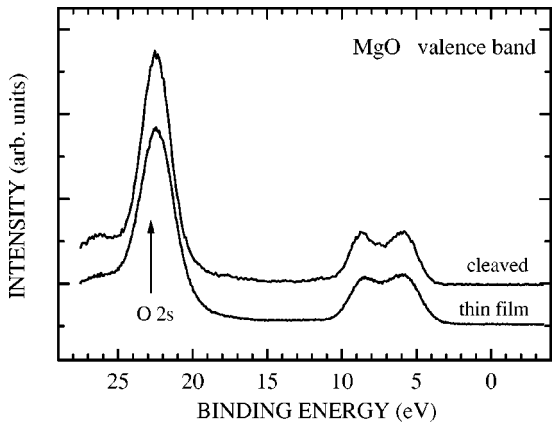

FIG. 2. Valence-band XPS spectra measured from a cleaved MgO single crystal (top), and from an 80-Å-thick MgO film grown on polycrystalline Al (bottom). Note the close similarity between the two spectra.

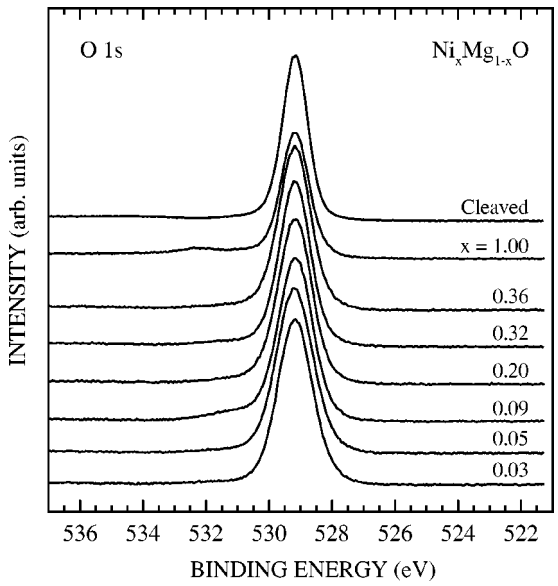

FIG. 3. O 1*s* core-level XPS spectra measured from the $Ni_xMg_{1-x}O$ films on Ag(100), as a function of *x*, aligned in energy to the O 1*s* spectrum of the *in situ* cleaved NiO sample (top most curve).

trum, despite the fact that the probing depth of about 15–20 Å is much smaller than the film thickness. This is due to the very high photoionization cross section of Ag 4*d* as compared to those of O 2*p*, Ni 3*d*, and Al 3*s*,3*p*. For comparison, we have also included in the top panel of the same figure the spectrum for the *in situ* cleaved NiO single crystal. The two spectra are indeed nearly identical. Moreover, the zero intensity at the Fermi level clearly demonstrates that the oxygen pressure used during the film growth was sufficient to fully oxidize Ni to NiO, and that the formation of Ni metal cluster during the growth of the NiO, as well as $Ni_xMg_{1-x}O$ films, did not take place. In Fig. 2 we show the valence band XPS spectrum of a 80-Å-thick MgO film on Al (bottom panel) together with that of the MgO single crystal (top panel). Also here the thin film and the single-crystal spectra are nearly identical, demonstrating the high chemical purity of the film.

Having verified the conditions for the growth of stoichiometric NiO and MgO thin films, epitaxially on the Ag(100) substrate[48–50] and in polycrystalline form on Al substrates, it is then possible to prepare *in situ* epitaxial $Ni_xMg_{1-x}O$ overlayers on Ag(100) with $0.03<x<1$, since NiO makes solid solutions with MgO over the entire range of nickel ion concentrations.[51] In Fig. 3 we report the O 1*s* spectra measured from the $Ni_xMg_{1-x}O$ films on Ag(100), as a function of the Ni concentration. For $0.09<x<1$, the peak position is about 529.1 eV, i.e., the same as in the cleaved NiO spectrum (top most curve). For $x=0.05$ and $x=0.03$, however, the O 1*s* is found at about 1 eV higher binding energy. Since there are no charging effects for MgO thin films on Ag(100),[48,49] we attribute this core-level shift to the different pinning of the chemical potential inside the oxide energy gap, which is expected to be different for high and low Ni concentrations. We remark that the full width at half maximum (FWHM) of the O 1*s* is found to be essentially constant for all values of *x*, and equal to the value measured for a 40-Å-thick MgO film on Ag(100),[48] confirming the absence of charging problems in the $Ni_xMg_{1-x}O$ overlayers on the Ag(100) substrate. The good quality of our spectra is also demonstrated by fact that the O 1*s* XPS peaks are very narrow, namely 0.9–1.3 eV. For a better comparison of the core-level spectra measured at different Ni concentrations, we have rigidly shifted all the XPS spectra to align the O 1*s* peak position with that of the cleaved NiO sample, as shown in Fig. 3. The value of the shifts, as well as the FWHM of the O 1*s* peaks as a function of *x*, are listed in Table I. Apart from the rigid energy shift, the O 1*s* spectra of $Ni_xMg_{1-x}O$ on Ag(100) do not show any dependence on *x*, and consist of a single Gaussian-like peak.

In Fig. 4 we report the Ni 2*p* spectra measured from $Ni_xMg_{1-x}O$ films on Ag(100), with $0.03<x<1$. The spectrum for $x=1$ (pure NiO) is essentially identical to the Ni 2*p* of the cleaved NiO single crystal (topmost curve) and, in

TABLE I. Full widths at half maximum (FWHM) of the Ni 2*p* and O 1*s* XPS core levels of $Ni_xMg_{1-x}O$ films on Ag(100), as a function of *x*. The thickness of the films as well as the rigid shift applied to all the core levels in order to align the peak position of the O 1*s* to that of the cleaved NiO single crystal are also listed.

		Cleaved	$x=1.00$	$x=0.36$	$x=0.32$	$x=0.20$	$x=0.09$	$x=0.05$	$x=0.03$
FWHM Ni $2p_{3/2}$	(eV)	3.2	3.4	3.0	2.8	2.5	2.2	1.9	1.7
FWHM Ni $2p_{1/2}$	(eV)	5.2	5.2	4.0	3.6	3.5	3.2	2.6	2.4
FWHM O 1*s*	(eV)	0.9	1.0	1.2	1.2	1.2	1.3	1.3	1.3
Shift	(eV)	0	0	0	0	0	−0.1	−1.1	−0.8
Thickness	(Å)		120	40	80	80	40	80	40

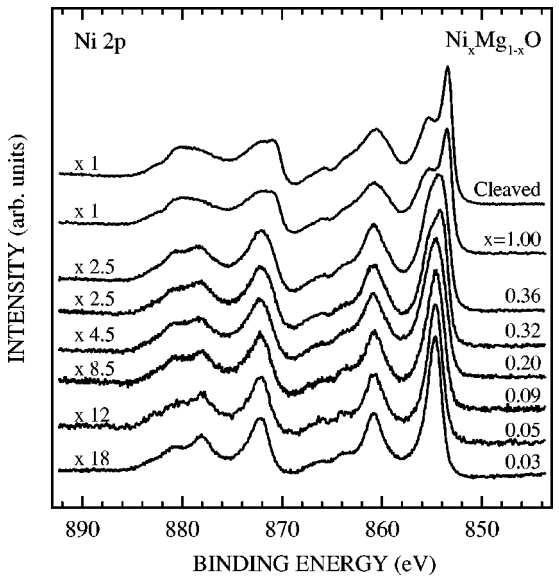

FIG. 4. Ni $2p$ core-level XPS spectra measured from $Ni_xMg_{1-x}O$ films on Ag(100), as a function of x. The spectra were shifted in energy so that the O $1s$ spectra are aligned to that of the *in situ* cleaved NiO sample (top most curve).

particular, exhibits the characteristic double peak $2p_{3/2}$ and $2p_{1/2}$ main lines of bulk NiO. For $x<1$, however, dramatic line-shape changes occur in the spectra. At $x=0.36$, both the $2p_{3/2}$ and $2p_{1/2}$ main lines consist of a single peak positioned around the centroid of the bulk main lines, at about 855 and 872 eV, respectively. For $x<0.36$, the position of these two peaks remains unchanged, and any further reduction of the nickel concentration only results in a monotonic decrease of the peak width (see Table I). The smallest FWHM of the $2p_{3/2}$ line is measured for $x=0.03$, namely 1.7 eV, that is almost half of the width of the bulk $2p_{3/2}$ line (FWHM=3.2 eV). The smallest FWHM of the $2p_{1/2}$ line is also measured for $x=0.03$, namely 2.4 eV. A similar narrowing with Ni dilution can also be observed for the $2p_{3/2}$ and $2p_{1/2}$ satellite structures in the energy range of 858–869 eV and 876–890 eV, respectively.

IV. DISCUSSION

In going from NiO as bulk material to NiO as an impurity in a MgO matrix, the Ni $2p$ XPS line shape changes dramatically. The double peak structure of the main line (FWHM=3.2 eV) collapses into a single peak upon dilution and the width of this peak is the smallest for the most dilute system (FWHM=1.7 eV, see Fig. 4 and Table I). We note that the FWHM of this narrow peak is much smaller than those reported earlier for the $Ni_xMg_{1-x}O$ $(0.09<x<0.47)$ powders[46] and for the $Ni_{0.1}Mg_{0.9}O$ sample.[4,42] Since in our spectra the FWHM is still decreasing when going from $x=0.05$ to $x=0.03$, and since with $x=0.03$ the probability[47] for two Ni ions in $Ni_xMg_{1-x}O$ to be neighbors with 180° Ni-O-Ni bond angle is about 15%, we conclude that the main line Ni $2p$ XPS of a single NiO impurity in MgO is probably even narrower than 1.7 eV.

For a more detailed look, we have replotted the spectra of the bulk and the most diluted NiO system together in the top panel of Fig. 5 after having applied a common integral-

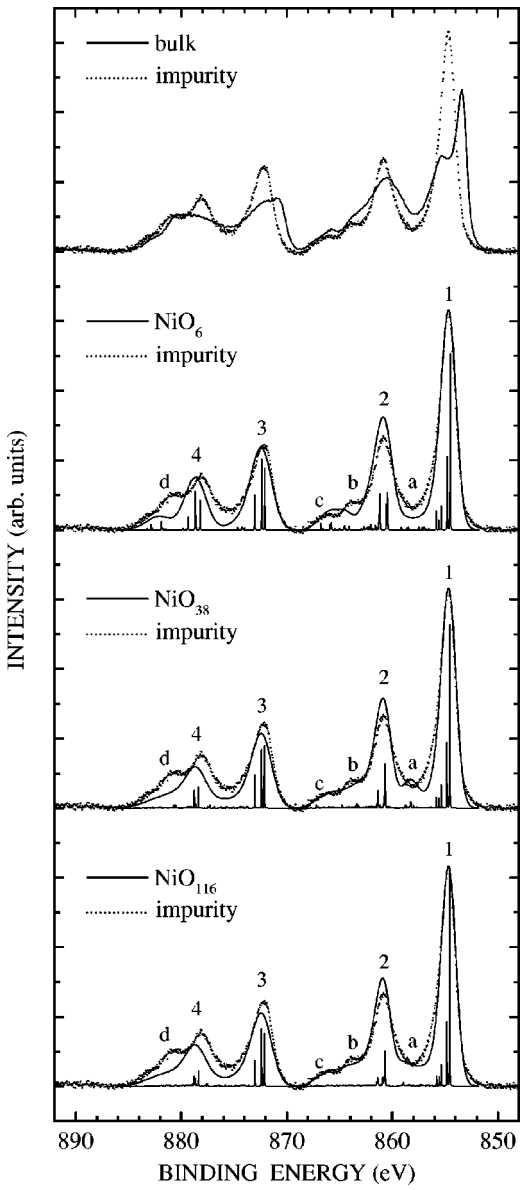

FIG. 5. Comparison between the experimental Ni $2p$ core-level XPS spectrum of the $Ni_{0.03}Mg_{0.97}O$ film on Ag(100) and the theoretical spectra calculated for a NiO_6, NiO_{38}, and NiO_{118} cluster. A Gaussian broadening with $\sigma=0.65$ eV (0.9 eV) for the $2p_{3/2}$ ($2p_{1/2}$) region has been used in the calculations. In the top panel the spectrum of the $Ni_{0.03}Mg_{0.97}O$ film is compared to that of the cleaved NiO single crystal.

background correction. The large differences between the two systems are evident. While the nonlocal screening model can explain why the Ni $2p$ main line of bulk NiO has a double peak and that of an impurity a single peak, the calculations reported so far[24,32] have neglected completely the multiplet effects for $2p^5 3d^n$ configurations, crucial for the understanding of the overall spectral line shape.[2,3] It is therefore important to show at least that even inclusion of the full multiplet structure cannot reproduce the bulk NiO spectrum if one uses a single-Ni-site model. While such a negative proof is difficult to give, an alternative is to demonstrate that the single-site model can accurately describe the experimentally observed spectrum for the diluted NiO system.

In calculating the Ni $2p$ electron removal spectra, we start

with a cluster consisting of a single Ni^{2+} ion surrounded by 6 O^{2-} ions in octahedral symmetry. The model Hamiltonian includes the full degeneracy of the Ni $3d$ and O $2p$ orbitals, as well as all on-site Ni $3d$-$3d$, Ni $2p$-$3d$, and O $2p$-$2p$ multiplet interactions. The model takes into account all nearest-neighbor Ni $3d$-O $2p$ and O $2p$-O $2p$ transfer integrals plus an octahedral crystal-field splitting for the Ni $3d$. This model Hamiltonian is the same as the one used to calculate the (resonant) $3d$, $3p$, and $3s$ photoemission spectra of a wide range of $3d$ TM oxides.[52]

The result for the NiO_6 cluster is shown in the second panel of Fig. 5. Here we have used the same parameter values as those determined from a detailed analysis of the (resonant) valence-band photoemission spectra of NiO.[52,53] The most relevant parameter, namely the O $2p$-Ni $3d$ charge-transfer energy Δ, is given essentially by the constraint that the calculation is to reproduce the 4-eV band gap of NiO correctly. A comparison with the measured spectrum of $Ni_{0.03}Mg_{0.97}O$ reveals that the cluster model reproduces the main features of the $2p$ spectrum, labeled as ''1,'' ''2,'' ''3,'' and ''4'' in the figure. Indeed, the single-site calculation gives a single peak for the main line for the diluted NiO and not the double peak observed for bulk NiO. There are, however, also features in the diluted NiO spectrum that cannot be reproduced, such as the intensity in the valley labeled ''a'' and the peak labeled ''b.'' Varying the paramater values does not provide a better overall fit.

To investigate the possible role of the O $2p$ band structure on the spectra,[41] we now also include the next shell of oxygen ions surrounding the NiO_6 cluster, i.e., we calculate the spectrum for a NiO_{38} cluster using the same set of parameter values. The third panel of Fig. 5 shows that there is now more intensity in the calculated spectrum in the region of valley ''a'' and peak ''b.'' While this is an improvement compared to the NiO_6 calculation, it also shows that the spectrum is quite sensitive to the band structure of the O $2p$, especially since the calculation produces a peak in valley ''a.''

As a next step to incorporate the oxygen band structure more properly, we add yet another shell of oxygen ions and calculate the spectrum for a NiO_{116} cluster. We are now very close to an Anderson impurity calculation that includes a realistic band structure for the O $2p$ host, since the O $2p$-O $2p$ transfer integrals used here reproduces well the valence band of MgO.[54] The bottom panel of Fig. 5 shows that the fit to the experimental spectrum is getting better: the intensity in valley ''a'' is now well reproduced.

Despite the good overall agreement between the calculated and the experimental impurity spectra, the quality of the experimental data is such that small discrepancies are easily recognizable. For example, the peak labeled ''d'' is still missing in the calculated spectrum, and also the calculated position of peak ''4'' is off by about 1 eV. Perhaps the polarization of the anions surrounding a core ionized metal atom, with the consequent formation of excitons on the ligands, can be included explicitly, since this process is known to produce high-energy satellites in early transition-metal oxides.[55] Another very interesting option is to include configuration dependent transfer integrals. It has been pointed out by Gunnarsson and Jepsen,[56] that the radial extent of atomiclike orbitals, and thus also the hopping matrix elements, depends strongly on the occupancy of this orbital, and on whether or not a core hole is present. Okada and Kotani[57] have investigated the consequences of this dependence for the interpretation of core-level spectra of transition-metal compounds, and have also been quite successful in reproducing the Ni $2p$ spectrum of $NiCl_2$ accurately.

One of the shortcomings that emerges from $2p$ core-level XPS studies so far, is that the calculated values for the charge-transfer energy Δ in TM and high-T_c compounds are systematically lower than the values needed to obtain the correct magnitude of the band gap. One reason could be that the transfer integrals depend on whether or not a core hole is present, and on the occupation of the orbital. Using this approach, Okada and Kotani[57] were able to obtain reasonable fits for the Ni $2p$ XPS spectra in Ni dihalides using Δ values that are consistent with the gap. Another reason is that most of the analyses have been carried out using a single-site ansatz, while in the systems considered, like NiO, strong inter-TM-site charge fluctuations are likely to be present. In our case, in which we analyze the dilute NiO system with the single-site Anderson-impurity-like model, we are indeed able to obtain good agreement between the experimental and calculated $2p$ core-level spectra, using parameter values that are consistent with the size of the band gap and with other spectroscopies as well.[52]

Our finding that the dilute NiO $2p$ XPS spectrum is well reproduced using an Anderson-impurity-like model, provides strong support for the idea that nonlocal screening processes are responsible for the double peak structure of the main line of the bulk NiO spectrum. It now becomes also clear why the Ni $2p$ XPS spectrum of Ni dihalides show a single peak for the main line which can be well explained using single-site approaches.[2,3,57] While in bulk NiO each Ni ion is surrounded by six Ni ions with 180° Ni-O-Ni bond angle and 12 Ni ions with 90°, in the dihalides each Ni ion is surrounded only by six Ni ions with 90° Ni-halogen-Ni bond angle. Realizing also that the largest transfer integral belongs to the 180° bonds, one can expect that inter-Ni-site hopping processes are very strongly reduced in the dihalides. It is therefore not surprising that the Ni $2p$ XPS spectra of $NiCl_2$ or $NiBr_2$ (see Ref. 7) show more similarities with the diluted NiO than the bulk NiO spectrum. Moreover, the fact that the Slater-Koster parameters $(pd\sigma)$ and $(pd\pi)$ are also smaller in the dihalides than in NiO[2] helps to make the dihalides look more like an impurity system. In comparing La_2NiO_4 with NiO, one observes that the main line of the Ni $2p$ spectrum of the nickelate is sharper.[42,58] This is also consistent with the nonlocal screening model. In the nickelate, each Ni ion is surrounded by four Ni ions with a 180° Ni-O-Ni bond angle and by none with the 90° bond angle. This also constitutes a reduction of the effective inter-Ni-site hopping process as compared to bulk NiO. Important is that the width of the Ni $2p_{1/2}$ main line in the nickelate (FWHM=3.0–3.5 eV, see Refs. 42 and 58) is still larger than that of the most diluted NiO in MgO system (FWHM=2.4 eV, see Table I), consistent with the fact that the presence of four Ni neighbors in the nickelates allows for inter-Ni-site hopping processes.

The double peak structure in the $2p$ main line of bulk NiO was ascribed to the presence of two types of states, namely one of mainly $2p^5 3d^{n+1}\underline{L}$ character for the lower

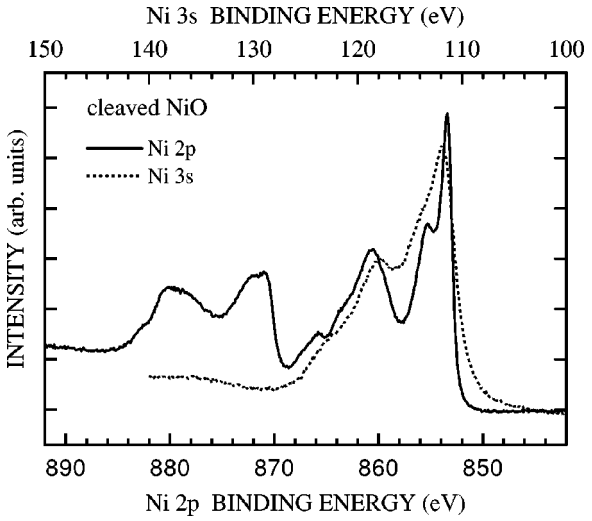

FIG. 6. Ni $3s$ and $2p$ core-level XPS spectra of an *in situ* cleaved NiO single crystal. The two spectra are plotted on the same eV/inch scale for the energy axis.

binding energy peak and another of mainly $2p^5 3d^{n+1}$ where the ligand hole is transferred from the core ionized site to the next-neighbor cluster, for the higher binding energy peak.[24] Whether one should follow this one-to-one assignment literally[4] is, however, questionable since the analysis was made without the inclusion of the full orbital degeneracy and multiplet interactions, while such is expected to affect the details of the line shape considerably.[33] In addition, our spectra show that the single peak main line of the diluted NiO system is positioned around the centroid of the double peak main line of bulk NiO, suggesting that, within this two-state assignment, the two states are degenerate in energy and that the two peaks in bulk NiO have in fact about equal amounts of local and nonlocal character.

It was on the basis of the Ni $3s$ XPS analysis of bulk NiO that Sangaletti, Depero, and Parmigiani[42] concluded that nonlocal screening effects are not needed to explain the spectra and that perhaps these effects are even nonexistent in Ni^{2+} compounds. They were able to reproduce the $3s$ spectra quite well using a single-site Anderson impurity model. Calculations by Atanasov and Reinen,[32] on the other hand, predict that the Ni $3s$ spectrum for a NiO impurity is different from that for a system in which nonlocal screening effects are present. In Fig. 6 we present bulk NiO $3s$ and $2p$ spectra which were taken under identical conditions of the *in situ* cleaved NiO single crystal. The line shapes of the spectra are quite different due to differences in the $3s$-$3d$ and $2p$-$3d$ multiplet interactions, leading to different multiplet structures and satellite intensities, as well as due to different lifetime broadenings. The important point of the comparison is that all in all the features in the $3s$ spectrum are much broader than those in the $2p$. It is therefore likely that this broadening will wash out the differences between an impurity and a bulk system. Perhaps one has to conclude that $3s$ XPS is not as informative as the $2p$ with regard to the nonlocal screening issue.

V. CONCLUSIONS

We have presented a high-resolution core-level XPS study of $Ni_xMg_{1-x}O$ crystals with $0.03<x<1$. We have shown that in bulk NiO the intersite interactions between neighboring Ni ions have a strong influence on the $2p$ core-level line shape, particularly in the region of the main lines, whereas in the dilute limit the core-level spectra are properly described by an Anderson impurity Hamiltonian provided it includes a realistic band structure for the O $2p$. Moreover, it is only in this limit that a single-site model can explain the core-level and valence-band spectra, as well as the optical data, by using one consistent set of parameter values. These results consolidate the concept of nonlocal screening, strongly supporting the existence and importance of intersite charge-transfer excitations, and provide an important contribution to the understanding of the electronic structure of NiO and other strongly correlated materials.

ACKNOWLEDGMENTS

We would like to thank A. Heeres, J. C. Kappenburg, and H. J. Bruinenberg for their skillful technical assistance. We would like to acknowledge L. Venema for providing the Ag(100) single crystal and M. Mulder for the RHEED gun used for the film thickness calibration. This work is supported by the Netherlands Foundation for Fundamental Research on Matter (FOM) with financial support from the Netherlands Organization for Scientific Research (NWO). S.A. acknowledges financial support by the European Union under Contract No. ERBCHBGCT930415. The research of L.H.T. has been made possible by financial support from The Royal Netherlands Academy of Arts and Sciences.

[1] *Core-Level Spectroscopy in Condensed Systems*, edited by J. Kanamori and A. Kotani (Springer-Verlag, Berlin, 1988).
[2] K. Okada and A. Kotani, J. Phys. Soc. Jpn. **60**, 772 (1991).
[3] K. Okada and A. Kotani, J. Phys. Soc. Jpn. **61**, 4619 (1992).
[4] S. Hüfner, Adv. Phys. **43**, 143 (1994).
[5] S. Hüfner, *Photoelectron Spectroscopy* (Springer-Verlag, Berlin, 1995).
[6] G. van der Laan, C. Westra, C. Haas, and G.A. Sawatzky, Phys. Rev. B **23**, 4369 (1981).
[7] J. Zaanen, C. Westra, and G.A. Sawatzky, Phys. Rev. B **33**, 8060 (1986).
[8] J. Park, S. Ryu, M. Han, and S.-J. Oh, Phys. Rev. B **37**, 10 867 (1988).
[9] A.E. Bocquet, T. Saitoh, T. Mizokawa, and A. Fujimori, Solid State Commun. **83**, 11 (1992).
[10] O. Gunnarsson and K. Schönhammer, Phys. Rev. B **23**, 4315 (1983).
[11] A. Kotani, H. Mizuto, T. Jo, and J.C. Perlebas, Solid State Commun. **53**, 805 (1985).
[12] J.C. Fuggle, O. Gunnarsson, G.A. Sawatzky, and K. Schonhammer, Phys. Rev. B **37**, 1103 (1988).
[13] H. Ogasawara, A. Kotani, R. Potze, G.A. Sawatzky, and T. Thole, Phys. Rev. B **44**, 5465 (1991).
[14] A. Fujimori, E. Takayama-Muromachi, Y. Uchida, and B. Okai,

Phys. Rev. B **35**, 8814 (1987).
[15] Z.X. Shen, J.W. Allen, J.J. Jeh, J.-S. Kang, W. Ellis, W. Spicer, I. Lindau, M.B. Maple, Y.D. Dalichaouch, M.S. Torikachvili, J.Z. Sun, and T.H. Geballe, Phys. Rev. B **36**, 8414 (1987).
[16] P. Steiner, V. Kinsinger, I. Sander, B. Siegwart, S. Hüfner, C. Politis, R. Hoppe, and H.P. Müller, Z. Phys. B: Condens. Matter **67**, 497 (1987).
[17] M. De Santis, A. Bianconi, A. Clozza, P. Castrucci, A. Di Cicco, M. De Simone, A.M. Flank, P. Lagarde, J. Budnick, P. Delogu, A. Gargano, R. Giorgi, and T.D. Makris, in *Proceedings of the International Symposium on the Electronic Structure of High-T_c Superconductors, Rome 1988*, edited by A. Bianconi and A. Marcelli (Pergamon, Oxford, 1989).
[18] J. Ghijsen, L.H. Tjeng, J. van Elp, H. Eskes, J. Westerink, G.A. Sawatzky, and M.T. Czyzyk, Phys. Rev. B **38**, 11 322 (1998).
[19] D.D. Sarma and A. Taraphder, Phys. Rev. B **39**, 11 570 (1989).
[20] K.S. Kim and R.E. Davis, J. Electron Spectrosc. Relat. Phenom. **1**, 251 (1972).
[21] M. Oku, H. Tokuda, and K. Hirokawa, J. Electron Spectrosc. Relat. Phenom. **53**, 201 (1991).
[22] St. Uhlenbrock, Chr. Scharfschwerdt, M. Neumann, G. Illing, and H.-J. Freund, J. Phys.: Condens. Matter **4**, 7973 (1992).
[23] A.E. Bocquet, T. Mizokawa, A. Fujimori, M. Matoba, and S. Anzai, Phys. Rev. B **52**, 13 838 (1995).
[24] M.A. van Veenendaal and G.A. Sawatzky, Phys. Rev. Lett. **70**, 2459 (1993).
[25] M.A. van Veenendaal, H. Eskes, and G.A. Sawatzky, Phys. Rev. B **47**, 11 462 (1993).
[26] H. Eskes and G.A. Sawatzky, Phys. Rev. Lett. **61**, 1415 (1988).
[27] F.C. Zhang and T.M. Rice, Phys. Rev. B **37**, 3759 (1988).
[28] D. Alders, F.C. Voogt, T. Hibma, and G.A. Sawatzky, Phys. Rev. B **54**, 7716 (1996).
[29] R. Neudert, T. Böske, O. Knauff, M. Knupfer, M.S. Golden, G. Krabbes, J. Fink, H. Eisaki, and S. Uchida, Physica B **230**, 847 (1997).
[30] T. Böske, O. Knauff, R. Neudert, M. Kielwein, M. Knupfer, M.S. Golden, J. Fink, H. Eisaki, S. Uchida, K. Okada, and A. Kotani, Phys. Rev. B **56**, 3438 (1997).
[31] T. Böske, K. Maiti, O. Knauff, K. Ruck, M.S. Golden, G. Krabbes, J. Fink, T. Osafune, N. Motoyama, H. Eisaki, and S. Uchida, Phys. Rev. B **57**, 138 (1998).
[32] M. Atanasov and D. Reinen, J. Electron Spectrosc. Relat. Phenom. **86**, 185 (1997).
[33] K. Okada and A. Kotani, Phys. Rev. B **52**, 4794 (1995).
[34] K. Okada and A. Kotani, J. Electron Spectrosc. Relat. Phenom. **78**, 53 (1996).
[35] K. Okada and A. Kotani, J. Phys. Soc. Jpn. **66**, 341 (1997).
[36] K. Okada and A. Kotani, Physica B **237-238**, 383 (1997).
[37] K. Okada and A. Kotani, J. Phys. Soc. Jpn. **68**, 666 (1999).
[38] A. Tanaka and T. Jo, J. Phys. Soc. Jpn. **65**, 912 (1996).
[39] A. Tanaka and T. Jo, Physica B **237-238**, 385 (1997).
[40] K. Karlsson, O. Gunnarsson, and O. Jepsen, Phys. Rev. Lett. **82**, 3528 (1999).
[41] K. Karlsson, O. Gunnarsson, and O. Jepsen, J. Phys.: Condens. Matter **4**, 2801 (1992).
[42] L. Sangaletti, L.E. Depero, and F. Parmigiani, Solid State Commun. **103**, 421 (1997).
[43] P.S. Bagus, G. Pacchioni, and F. Parmigiani, Chem. Phys. Lett. **207**, 569 (1993).
[44] F. Parmigiani and L. Sangaletti, Chem. Phys. Lett. **213**, 613 (1993).
[45] L. Sangaletti, L.E. Depero, P.S. Bagus, and F. Parmigiani, Chem. Phys. Lett. **245**, 463 (1995).
[46] M. Oku and K. Hirokawa, J. Electron Spectrosc. Relat. Phenom. **10**, 103 (1977).
[47] For randomly distributed Ni ions in $Ni_xMg_{1-x}O$, a Ni ion may have n ($n=1,\ldots,6$) Ni ions as neighbors, with a probability given by the Poisson distribution $[z!x^n(1-x)^{z-n}]/[(z-n)!n!]$, where z is the coordination number.
[48] S. Altieri, L.H. Tjeng, F.C. Voogt, T. Hibma, and G.A. Sawatzky, Phys. Rev. B **59**, R2517 (1999).
[49] S. Altieri, L.H. Tjeng, F.C. Voogt, T. Hibma, O.C. Rogojanu, and G.A. Sawatzky (unpublished).
[50] F.C. Voogt, S. Altieri, O.C. Rogojanu, and T. Hibma (unpublished).
[51] S. Holgersson and A. Karlsson, Z. Anorg. Allg. Chem. **182**, 255 (1929).
[52] A. Tanaka and T. Jo, J. Phys. Soc. Jpn. **63**, 2788 (1994).
[53] The parameter values adopted in the model are $\Delta=4.7$ eV, $U_{3d3d}=7.3$ eV, $U_{2p3d}=8.5$ eV, $U_{2p2p}=5.0$ eV, $pd\sigma=-1.27$ eV, $pd\pi=0.55$ eV, $pp\sigma=0.55$ eV, $pp\pi=-0.15$ eV, $10Dq=0.7$ eV, with the Slater integrals given by 80% of their Hartree-Fock values and the Ni ξ_{2p} and ξ_{3d} by the full Hartree-Fock values. All Δ and U values are given with respect to the multiplet average.
[54] L.H. Tjeng, M.B.J. Meinders, and G.A. Sawatzky, Surf. Sci. **236**, 341 (1990).
[55] D.K.G. de Boer, C. Haas, and G.A. Sawatzky, Phys. Rev. B **29**, 4401 (1984).
[56] O. Gunnarsson and O. Jepsen, Phys. Rev. B **38**, 3568 (1988).
[57] K. Okada and A. Kotani, J. Electron Spectrosc. Relat. Phenom. **71**, R1 (1995).
[58] H. Eisaki, S. Uchida, T. Mizokawa, H. Namatame, A. Fujimori, J. van Elp, P. Kuiper, G.A. Sawatzky, S. Hosoya, and H. Katayama-Yoshida, Phys. Rev. B **45**, 12 513 (1992).